

## Stochastic resonance in threshold systems

M. M. Alibegov\*

*Institute of Applied Geophysics, Moscow, Russia*

(Received 19 May 1998; revised manuscript received 9 October 1998)

We consider signal processing in simple threshold systems with nonstationary additive and/or multiplicative noise. A discrete-time process with a small periodical signal masked by noise represents an input. The systems convert sampled input data to a nonstationary random point event flow carrying some information on an input signal. As it is shown in our previous study [M.M. Alibegov, *Astron. Lett.* **22**, 564 (1996)], the Rayleigh spectral function of a random point event train estimates a signal-to-noise ratio (SNR) at selected frequencies. Based on these results, we compute a system response at signal frequencies as a function of threshold and input noise intensity. The threshold systems are shown to reveal stochastic resonance (SR), i.e., output SNR exhibits a maximum at resonant noise intensity (intensities) and threshold(s) at rather common conditions. We show that SR and Rayleigh spectral technique allow us to carry out numerical signal detection in data sets with noise. [S1063-651X(99)06704-5]

PACS number(s): 05.40.-a, 02.50.-r, 07.05.Kf

### I. INTRODUCTION

The performance of any complex system depends on a correct information exchange between its components. In most natural and man-made systems, a signal carrying information is often mixed with noise. Usually noise contamination makes it difficult to detect signals, but in some cases the effect known as stochastic resonance (SR) improves conditions for signal detection when noise and system parameters become “optimal.” In this effect noise comes out as a carrier of information and plays a positive role. After the first publications in 1981 and 1982 [1], SR gained a certain popularity in physics, chemistry, biology, and technology (see reviews [2,3]). The signature of SR is that the output signal-to-noise ratio (SNR) has a sharp maximum at optimal input noise intensity  $\sigma_{opt}$ , and is zero if noise is absent or very large (i.e., the system exhibits “a resonance response”). Wiesenfeld and Moss [3] noted a remarkable similarity of the responses for all three main types of SR—the bistable potential model, the fire-and-reset excitable system model, and a simple threshold model. The approximate formula for the SNR illustrates this assertion:

$$\gamma \propto \left( \eta \frac{s}{\sigma} \right)^2 \exp\left( -\frac{s}{\sigma} \right), \quad (1)$$

where  $\gamma$  is the output SNR,  $\eta$  is the input signal strength,  $\sigma$  is the input noise intensity, and  $s$  is a constant related to the barrier height or the threshold. Therefore, we hope that studying one of the SR models will help in understanding other related models better.

The theory of SR in simple threshold models was developed recently [4] for additive noise. The systems were fed by the input data set  $x_A(t)$  consisting of the sum of the periodical signal  $\alpha(t)$  and the Gaussian or uniform noise  $\xi$ :

$$x_A(t) = \alpha(t) + \xi. \quad (2)$$

Processes with multiplicative noise are less popular (see, e.g., [5]):

$$x_M(t) = \alpha(t)\xi, \quad (3)$$

where  $\bar{\xi} = 0$ .

Both processes can be described in terms of nonstationary input noise. Process (2) is represented by the noise model with the time-dependent mean  $\mu(t)$ , and process (3), by the noise model with the time-dependent variation  $\sigma^2(t)$ .

The purpose of this study is to develop a theory for SR in simple threshold models with discrete in time input for arbitrary distributed multiplicative and additive noise. Our approach uses the Rayleigh spectral technique instead of conventional methods based on the Fourier transform.

### II. RAYLEIGH POWER SPECTRA

We can describe a rather simple procedure to estimate SNR by using the results of our previous study [6]. The Rayleigh spectral function has been defined as

$$R(f) = N^{-1} \left[ \left( \sum_{j=1}^N \cos(2\pi f t_j) \right)^2 + \left( \sum_{j=1}^N \sin(2\pi f t_j) \right)^2 \right] \quad (4)$$

for a point event train  $\{t_j\}$ ,  $j = 1, 2, \dots, N$ . It has been found that if an event rate  $r(t)$  can be expanded in the series (for example, in the Fourier series),

$$r(t) = \frac{a_0}{2} + \sum a_k \cos(2\pi f_k t + \phi_k), \quad (5)$$

the averaged Rayleigh spectrum for the train  $\{t_j\}$  at the frequencies  $f_k \gg \Delta t^{-1}$  (where  $\Delta t$  is a length of the train):

(i) has peaks with the averaged amplitudes

$$\langle R(f_k) \rangle = 1 + \left( \frac{a_k}{a_0} \right)^2 (\langle N \rangle - 1) \approx 1 + \left( \frac{a_k}{a_0} \right)^2 \langle N \rangle, \quad (6)$$

where the angular brackets mean ensemble averaging; and

\*Electronic address: alibeg@glasnet.ru

(ii) the width of the averaged spectral peak is  $\Delta f_k = 2\Delta t^{-1}$ .

Taking into account that  $\langle N \rangle = \int_{\Delta t} r(t) dt = (a_0/2)\Delta t$ , Eq. (6) can be rewritten as

$$\langle R(f_k) \rangle \approx 1 + \frac{a_k^2}{2a_0} \Delta t. \quad (7)$$

By defining  $\text{SNR}(f_k) \equiv \gamma(f_k) \equiv a_k^2/2a_0$  (because  $a_0$  is a background noise rate, and  $a_k$  represents a signal amplitude), we obtain

$$\gamma(f_k) \equiv \frac{a_k^2}{2a_0} \approx \Delta t^{-1} (\langle R(f_k) \rangle - 1). \quad (8)$$

It is worth noting that there are no restrictions on a signal frequency, except evident  $f_k \gg \Delta t^{-1}$ .

### III. SNR AS A FUNCTION OF THRESHOLD AND NOISE

We consider a threshold system with a discrete in time input  $\{x_j\} = \{x(t_j)\}$ , e.g., sampled measurements of analog physical quantity. The samples assumed to be uniformly distributed in time, i.e., a sample interval can be either constant:  $x(t_m) = x(t_0 + m\delta t_0)$ ,  $\delta t_0 = \text{const}$ , or random, but with a constant mean value, i.e.,  $x(t_{m+1}) = x(t_m + \Delta t_m)$ ,  $\langle \Delta t_m \rangle = \delta t_0 = \text{const}$ . In both cases the mean input data rate is constant:  $\nu_0 = \delta t_0^{-1}$ . A system output is a time sequence of the moments,  $\{t_k\}$ , of measurements exceeding the threshold  $s$ :  $x(t_k) \geq s$  [see Fig. 1(a)]. Below we use the term ‘‘threshold crossing’’ to denote these events, and  $t_k$  is the threshold crossing time. In our model, if the system threshold  $s \rightarrow -\infty$ , then the output event rate is  $r \rightarrow \nu_0 = \text{const}$ , and hence, according to Eqs. (5) and (8),  $\text{SNR}(f) = 0$  at any frequency and with arbitrary distribution of  $x$ . If there are no signals in the input, i.e., only a stationary noise feeds the threshold system, then the mean distance between output events does not change in time with any threshold, and again  $r = \text{const}$ .

Let input measurements have the time-dependent distribution density function:  $f(x; \mu(t), \sigma(t))$ , where  $\mu$  and  $\sigma$  are parameters. We assume that  $f(x; \mu, \sigma) = f(x/\sigma; \mu/\sigma, 1)$ . For the sake of simplicity let us suppose that  $f(x; \mu, \sigma)$  is unimodal, i.e., it has one maximum. For example, the time-dependent Gaussian distribution density is

$$f_G(x; \mu(t), \sigma(t)) = \frac{1}{\sqrt{2\pi\sigma^2(t)}} \exp\left\{-\frac{[x - \mu(t)]^2}{2\sigma^2(t)}\right\}. \quad (9)$$

Since the probability of  $x$  being greater than or equal to a threshold  $s$  is  $\Pr(x \geq s) = \int_s^\infty f(x; \mu(t), \sigma(t)) dx$ , the mean threshold crossing rate is given by [see Fig. 1(a)]

$$r_s(t) = \nu_0 \int_s^\infty f(x; \mu(t), \sigma(t)) dx = \nu_0 F\left(\frac{s - \mu(t)}{\sigma(t)}\right), \quad (10)$$

where  $\nu_0$  is input event occurrence rate. It is easy to see that with a Gaussian-distributed signal,  $F_G(z) = 1/2 - [1/(2\sqrt{2})] \text{erf}(z)$ , where  $\text{erf}(z) = \sqrt{2} \int_{-z}^z f_G(x; \mu, \sigma) dx$  is the error function.

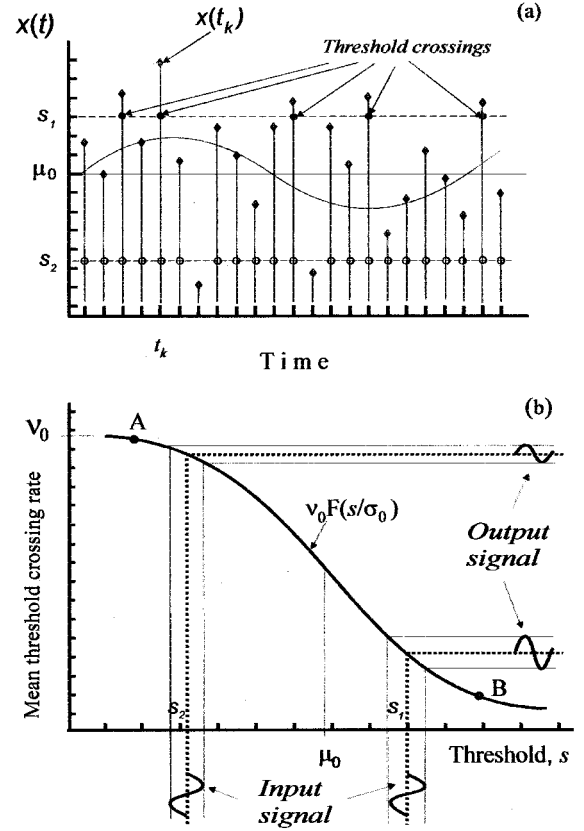


FIG. 1. (a) Threshold model with sinusoidal signal  $\mu(t) = \eta \cos(2\pi f_0 t)$  and the additive Gaussian noise as input. (b) The operational diagram of the threshold system. A conversion of input signal into an output modulated flow of point events. The device responds when its operational region is between points A and B of the curve  $F(s/\sigma_0)$ . The slope of a noise distribution function provides a noise distribution function provides signal amplification.

In our approach we assume the periodic signal is contained in the noise parameters  $\mu(t)$  and/or  $\sigma(t)$ . Our aim is to compute the response of the threshold systems, described above.

Consider two cases: the additive noise,

$$\sigma = \sigma_0 = \text{const}, \quad \mu(t) = \mu_0 + \eta \sin(2\pi f_A t + \phi_0); \quad (11)$$

and the multiplicative noise,

$$\sigma(t) = \sigma_0 + \eta \sin(2\pi f_M t + \phi_0), \quad \mu = \mu_0 = \text{const}, \quad (12)$$

where  $\eta/\sigma_0 \ll 1$  (weak signal), and  $\Delta t^{-1} \ll f_{A,M}$ . (To simplify our reasoning we assume  $f_{A,M} \ll \nu_0$ , keeping in mind that actually the restrictions are weaker.) Without loss of generality we suppose also  $\mu_0 = 0$  and  $\phi_0 = 0$ .

(a) *Additive noise.* The average output event rate (or threshold crossing rate) of the threshold system with the non-stationary noise under conditions (11) is

$$r_s(t) = \nu_0 \int_s^\infty f(x; \mu(t), \sigma_0) dx = \nu_0 F\left(\frac{s}{\sigma_0} - \frac{\eta}{\sigma_0} \sin(2\pi f_A t)\right). \quad (13)$$

We can expand Eq. (13) to first order by a Taylor expansion:

$$r_s(t) \approx \nu_0 \left[ F(s/\sigma_0) - \frac{\eta}{\sigma_0} F'(s/\sigma_0) \sin(2\pi f_A t) \right], \quad (14)$$

where  $F'(x) = dF(x)/dx$  is a derivative. From this expression it can be seen that the threshold system linearly converts a weak input signal to a changing output event rate. Figure 1(b) illustrates how this conversion is carried out. Substituting the coefficients of the expansion from Eq. (14) in Eq. (7) we obtain

$$\langle R(f_A) \rangle = 1 + \nu_0 \Delta t \frac{\left( \frac{\eta}{\sigma_0} \right)^2 F'^2(s/\sigma_0)}{4F(s/\sigma_0)} = 1 + \gamma_A(f_A) \Delta t, \quad (15)$$

and the output SNR for the additive noise case reads

$$\gamma_A(f_A) = \nu_0 \frac{\left( \frac{\eta}{\sigma_0} \right)^2 F'^2(s/\sigma_0)}{4F(s/\sigma_0)} = \nu_0 K_A(s, \sigma_0, f_A), \quad (16)$$

where  $K_A(s, \sigma_0, f_A)$  is the normalized dimensionless system response at a signal frequency. This quantity can be regarded also as a SNR per unit input rate. Equations (4), (8), and (16) show that  $K_A(s, \sigma_0, f_A)$  is easily estimated both theoretically and experimentally. To examine the correctness of our theory we have simulated the performance of the system as follows: (1) The consequence of Gaussian numbers  $\{x(t_j)\}, t_j = 1, \dots, N_0 = 3000$  has been generated. The numbers were distributed according to Eq. (9), where the signal frequency  $f_A = 0.04$  and signal amplitude  $\eta = 0.01$ . (2) The numbers exceeding some threshold value  $s$  have been selected; their moments of occurrence formed the point event train  $\{t_k\}_s, k = 1, 2, \dots, N$ . (3) The Rayleigh spectrum (4) of this train was computed in the range near the signal frequency. The strongest peak in this spectral range was assumed to estimate the experimental SNR<sub>A</sub> (or  $K_A$ ) for given threshold and noise. Peak values were averaged over 100 trials at each pair of  $s$  and  $\sigma_0$ . In Fig. 2 the results of simulations (symbols) are compared with the theoretical computations (solid lines).

(b) *Multiplicative noise.* The output averaged event rate (or threshold crossing rate) of the thresholds system with the nonstationary Gaussian noise (9) under conditions (12) is given by

$$r_s(t) = \nu_0 F(s/\sigma(t)) = \nu_0 F\left(\frac{s}{\sigma_0 + \eta \sin(2\pi f_0 t)}\right) \approx \nu_0 \left[ F(s/\sigma_0) - \frac{s\eta}{\sigma_0^2} F'(s/\sigma_0) \sin(2\pi f_0 t) \right]. \quad (17)$$

This equation shows that the signal is transformed to the output rate as above in the additive noise case (11). We again use Eqs. (8) and (17) to obtain SNR:

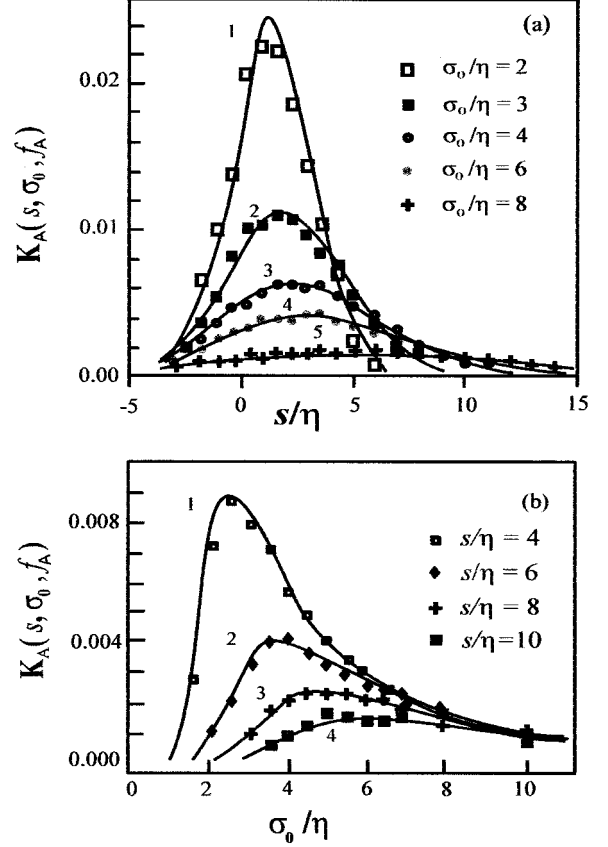


FIG. 2. Threshold model responses for additive noise with additive Gaussian noise input at the signal frequency  $f_A$ . (a) Normalized SNR (i.e.,  $K_A$ ) vs threshold  $s/\eta$  for different noise strength  $\sigma_0/\eta$ ; theory (solid lines): (1)  $\sigma_0/\eta = 2$ , (2)  $\sigma_0/\eta = 3$ , (3)  $\sigma_0/\eta = 4$ , (4)  $\sigma_0/\eta = 6$ , (5)  $\sigma_0/\eta = 8$ . (b) Normalized SNR (i.e.,  $K_A$ ) vs input noise strength  $\sigma_0/\eta$  for different thresholds  $s/\eta$ ; theory (solid lines): (1)  $s/\eta = 4$ , (2)  $s/\eta = 6$ , (3)  $s/\eta = 8$ , (4)  $s/\eta = 10$ . The symbols represent averaged maximal values of spectral peaks near signal frequency  $f_A$ . Statistical errors are within 30%.

$$\gamma_M(f_M) = \nu_0 \frac{\left( \frac{s}{\sigma_0} \right)^2 \left( \frac{\eta}{\sigma_0} \right)^2 F'^2(s/\sigma_0)}{4F(s/\sigma_0)} = \nu_0 K_M(s, \sigma_0, f_M). \quad (18)$$

The normalized system response  $K_M(s, \sigma_0, f_M)$  differs from  $K_A(s, \sigma_0, f_A)$  only by the factor  $(s/\sigma_0)^2$ . We again have simulated the system performance for the multiplicative case as described above. The results of simulations along with theoretical curves are presented in Fig. 3.

Equations (16) and (18) can be rewritten in the following way:

$$\gamma_A(f_A) = \nu_0 \left( \frac{\eta}{\sigma_0} \right)^2 Q(s/\sigma_0), \quad (19)$$

$$\gamma_M(f_M) = \nu_0 \left( \frac{s}{\sigma_0} \right)^2 \left( \frac{\eta}{\sigma_0} \right)^2 Q(s/\sigma_0), \quad (20)$$

where

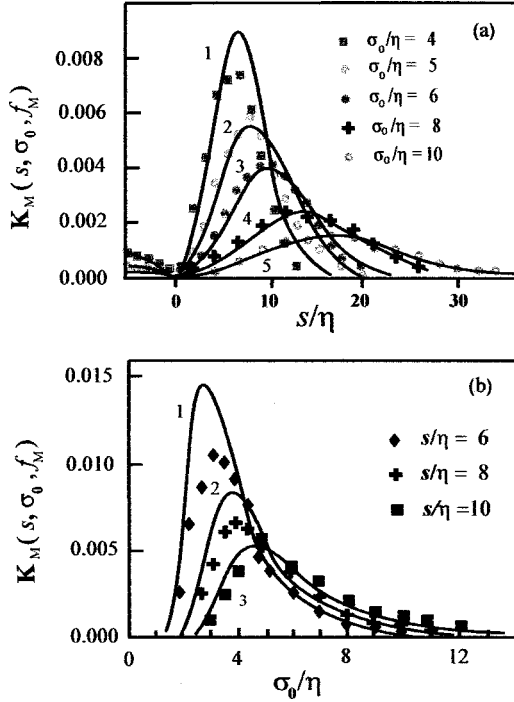


FIG. 3. Normalized (dimensionless) resonance characteristics,  $K_M(s, \sigma_0, f_M)$ , for threshold model with multiplicative Gaussian noise input at the signal frequency  $f_M$ . (a) Normalized SNR (i.e.,  $K_M$ ) vs threshold  $s/\eta$  for different noise strength  $\sigma_0/\eta$ ; theory (solid lines): (1)  $\sigma_0/\eta=2$ , (2)  $\sigma_0/\eta=3$ , (3)  $\sigma_0/\eta=4$ , (4)  $\sigma_0/\eta=6$ , (5)  $\sigma_0/\eta=8$ . (b) Normalized SNR (i.e.,  $K_M$ ) vs input noise strength  $\sigma_0/\eta$  for different thresholds  $s/\eta$ ; theory (solid lines): (1)  $s/\eta=4$ , (2)  $s/\eta=6$ , (3)  $s/\eta=8$ , (4)  $s/\eta=10$ . The symbols represent averaged maximal values of spectral peaks near signal frequency  $f_0$ . Statistical error is within 30%.

$$Q(s/\sigma_0) = \frac{F'^2(s/\sigma_0)}{4F(s/\sigma_0)}. \quad (21)$$

$Q(x/\sigma_0)$  can be treated as the generalized response of the threshold system. Using these equations we can predict a system's response for any noise distribution. Figure 4 reproduces  $Q(x/\sigma_0)$  according to Eq. (21) for the Gaussian (9) and uniform input distributions. Equations (19)–(21) show that the system responses  $K_{A,M}(s, \sigma_0, f_{A,M})$  together with the function  $Q(x/\sigma_0)$  become zero, at arbitrary noise distribution, when  $s/\sigma_0 \rightarrow \pm\infty$ . This implies that SNR's expose peaks at intermediate values of thresholds-to-noise ratios. Figure 1(b) shows that the resonance arises with any S-shaped noise distribution function, such as the Gaussian or uniform ones, due to its nonlinearity. The system response grows when a device operates in the steep section of the curve, and diminishes elsewhere. The device operational region depends on a threshold. Therefore the system response is small at low thresholds ( $s \rightarrow -\infty$ ). In the region *A-B* it grows to a maximum, and then decreases as the threshold keeps rising. This type of resonance has been described by Jang [4]. It happens when the noise is kept constant. The conventional SR arises in the systems with a fixed threshold. Figure 1(b) illustrates that at a strong noise ( $\sigma_0 \rightarrow \infty$ ) the slope of the curve becomes small as well as the system response. The response is also absent when there is no noise to

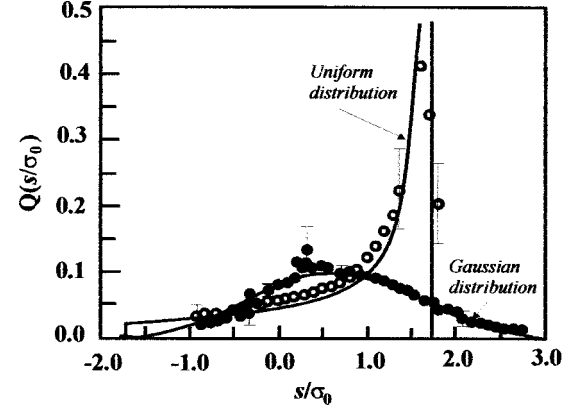


FIG. 4. Generalized responses  $Q$  vs  $s/\sigma_0$  for the Gaussian and uniform input noise distributions. Theoretical predictions according to Eq. (21) are shown with the solid lines. The filled circles are averaged experimental Gaussian data derived from those in Figs. 2 and 3. Empty circles denote results of the uniform noise simulations. (Multiplicative case points near  $s=0$  were missed.)

feed the device (i.e.,  $\sigma_0 \rightarrow 0$ ).  $F(s/\sigma_0)$  changes into the step function, and the output  $\text{SNR} \rightarrow 0$  unless  $s=0$ . The response grows in a relatively short intermediate interval of the noise intensity. Usually we can find the optimal values of  $s$  and  $\sigma_0$  by solving the equations

$$\begin{aligned} \frac{\partial}{\partial \sigma_0} K_{A,M}(s, \sigma_0) &= 0, \\ \frac{\partial}{\partial s} K_{A,M}(s, \sigma_0) &= 0. \end{aligned} \quad (22)$$

But sometimes it is easier to estimate these values numerically, using Eqs. (19)–(21). The simple analysis gives a general solution of Eq. (22): the optimal thresholds and fixed noise intensities are connected by the relation  $s_{opt} = k\sigma_0$ , where  $k$  is a constant, depending on the noise distribution and mode (additive or multiplicative). The relation between optimal noise intensities and fixed thresholds is not so simple.

Reasonings presented above remain true when input noise is colored and/or continuous. In that case a series of local maxima can be selected as a system input and the function  $f(x; \mu, \sigma)$  describes their probability distribution density, and our analysis is repeated. The parameter  $\nu_0$  is defined as a mean number of local peaks in a unit of time at extremely low threshold values:  $\nu_0 = r_{s \rightarrow -\infty}$ . Of course, it must be constant in the time interval  $\Delta t$ .

(c) *Note.* We have used equation  $F'_{G,U} \approx [F_{G,U}(s/\sigma_0 + \eta/\sigma_0) - F_{G,U}(s/\sigma_0 - \eta/\sigma_0)] / (2\eta/\sigma_0)$  instead of the formally correct equation  $F'_{G,U} = -f_{G,U}(s/\sigma_0, 0, 1)$  in the computation of the theoretical characteristics. Indexes *G* and *U* mean the Gaussian or uniform distributions. This approximation occurred to be more accurate at relatively large signal amplitudes.

#### IV. PERIODICAL SIGNAL DETECTION

Jung [4] has shown that there are optimal values for the threshold that yield optimal performance in the threshold

systems with the additive Gaussian input noise. We generalize this result to the threshold systems with multiplicative noise input and a wide range of noise distributions. Thus the system response SNR vs  $s$  with a maximum seems to be the signature of SR as well as conventional resonance curve SNR vs  $\sigma_0$ .

Our analysis shows that the output SNR exhibits a sharp maximum at optimal threshold-to-noise ratios, when the noise is kept constant. For example, the system with the Gaussian noise imposes the resonance, when  $s_{Aopt} \approx 0.62\sigma_0$ , and  $s_{Mopt} \approx 1.64\sigma_0$ , for the additive and multiplicative cases, respectively. A sharp maximum of SNR( $s$ ) allows one to use SR in optimization of the digital signal processing.

To demonstrate the SR and the Rayleigh spectral technique in a signal detection, a long consequence of random numbers has been generated. The numbers were distributed according to Eq. (9) with the time-dependent parameters  $\mu(t) = 0.2 \sin(2\pi f_A t)$  and  $\sigma(t) = 1 + 0.2 \sin(2\pi f_M t)$ , where  $\eta = 0.2$ ,  $f_A = 0.04$ , and  $f_M = 0.05$ . The consequence simulated a process with sinusoidal signals masked by the additive and multiplicative Gaussian noise.

The first step of the signal detection is to find reliable spectral peaks and then to estimate the system response [Fig. 5(a)]. There are two spectral peaks in our example, and two responses are estimated at the frequencies  $f_A$  and  $f_M$ . Their position and shape determine the noise modes (additive and multiplicative), distributions (Gaussian), optimal thresholds ( $s_{Aopt}$ , and  $s_{Mopt}$ ), signal amplitudes ( $\eta$ ), and noise standard deviation ( $\sigma = 1.61s_{Aopt} = 0.62s_{Mopt}$ ).

The second step is the analysis of Rayleigh spectra at the resonant thresholds [Fig. 5(b)]. It makes more precise an estimation of signal frequencies and amplitudes, and evaluates phases of signals [6].

Of course, we have described here a highly simplified procedure of signal detection. This approach sometimes has an advantage over conventional methods. For example, the signal at  $f_M$  could not be detected by the straightforward Fourier transform. Our method has shown good results in the detection of periodicities in solar activity indexes (e.g., [7]).

## V. CONCLUSION

We have presented the theory of SR in the simplest threshold systems with a discrete-time input, using the Rayleigh spectral technique. The system responses have been estimated when a weak periodical and noise-contaminated signal feeds the system at additive and multiplicative noise modes. We have studied in detail Gaussian and (in brief) uniform noise cases, and we expect good agreement with theory and experiment in the case of arbitrary noise distribution.

The system responses were shown to reveal peaks at op-

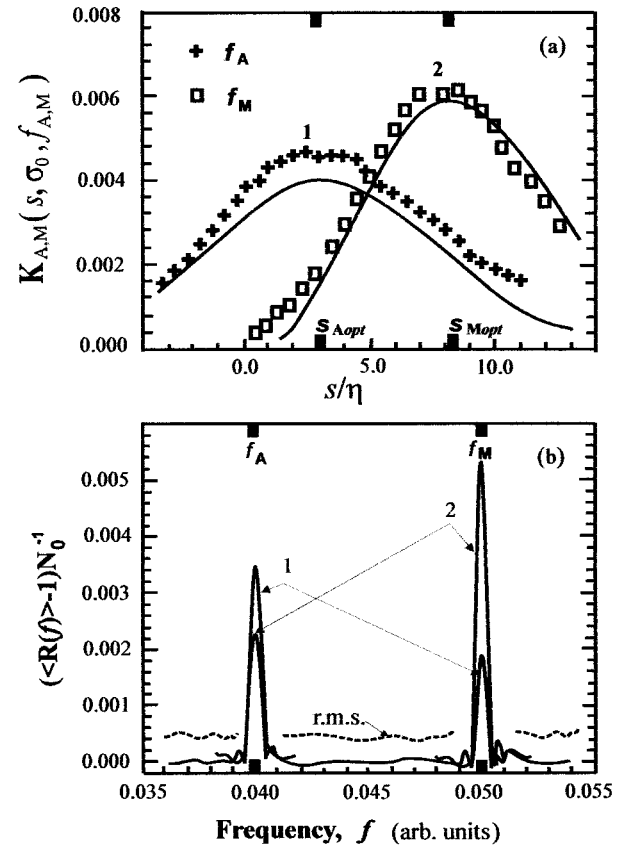


FIG. 5. Signal detection from the simulated data set. (a) The averaged resonance responses at signal frequencies: (1)  $f_A$ , (2)  $f_M$ . Solid lines are theoretical. (b) Averaged spectra of SNR at resonant thresholds (experimental). Statistical errors are within 30%.

timal values of noise intensity and threshold in a wide range of noise distributions. These values can be easily estimated. Thus, SR seems to be a rather common phenomenon in threshold devices.

The optimal parameters of the systems do not depend on a signal strength and frequency. Since the aperiodic signal can be treated as a process with a very large period, the aperiodic SR (or APS), introduced and developed recently [8], can apparently be described in terms of SNR as well as in terms of cross-correlation indexes  $C_0$  and  $C_1$ . The threshold system responses can be predicted from the known noise parameters, and vice versa.

Our results reveal the signal processing capabilities of the systems studied here. The proposed techniques (SR + the Rayleigh spectral method) could be used for estimating threshold model input parameters, such as signal frequencies, phases, amplitudes, noise intensity, and distribution. It could also be useful for the design of threshold devices, communication, and other applications.

- [1] A. Suter and A. Vulpiani, J. Phys. A **14**, L483 (1981); C. Nicolis, Tellus **34**, 1 (1982).  
 [2] A.R. Bulsara and L. Gammaitoni, Phys. Today **49** (3), 39 (1996); J. Stat. Phys. **70**, 1 (1993); Nuovo Cimento D **17**, 653 (1995); L. Gammaitoni, P. Hanggi, P. Jung, and F.

- Manchesoni, Rev. Mod. Phys. **70**, 223 (1998). See also the bibliography on SR at <http://www.pg.infn.it/sr/>  
 [3] K. Wiesenfeld and F. Moss, Nature (London) **373**, 33 (1995).  
 [4] Continuous input is considered in P. Jung, Phys. Lett. A **207**, 93 (1995); Z. Gingle, L.B. Kiss, and F. Moss, Europhys. Lett.

- 29**, 191 (1995); quantized input is analyzed in L. Gammaitoni, Phys. Rev. E **52**, 4691 (1995).
- [5] L. Gammaitoni, F. Marchesoni, E. Menichella-Saetta, and S. Santucci, Phys. Rev. E **49**, 4878 (1994); P.M. Gade, R. Rai, and H. Singh, *ibid.* **56**, 2518 (1997).
- [6] M.M. Alibegov, Pis'ma v Astron. Zh. **22**, 631 (1996) [Astron. Lett. **22**, 564 (1996)].
- [7] M.M. Alibegov, Pis'ma v Astron. Zh. **20**, 393 (1994) [Astron. Lett. **20**, 332 (1994)].
- [8] J.J. Collins, C.C. Chow, and T.T. Imhoff, Phys. Rev. E **52**, R3321 (1995); J.J. Collins, C.C. Chow, A.C. Capela, and T.T. Imhoff, *ibid.* **54**, 5575 (1996); J.J. Collins, T.T. Imhoff, and P. Crigg, *ibid.* **56**, 923 (1997).